

## Longitudinal monitoring of DNA viral loads in transplant patients using quantitative metagenomic next-generation sequencing

Ellen C. Carbo\*#, Anne Russcher\*, Margriet E.M. Kraakman, Caroline S. de Brouwer, Igor A. Sidorov, Mariet C.W. Feltkamp, Aloys C.M. Kroes, Eric C.J. Claas, Jutte J.C. de Vries

Clinical Microbiological Laboratory, department of Medical Microbiology, Leiden University Medical Center, Leiden, the Netherlands;

[E.C.Carbo@lumc.nl](mailto:E.C.Carbo@lumc.nl), [A.Russcher@meandermc.nl](mailto:A.Russcher@meandermc.nl), [M.E.M.Kraakman@lumc.nl](mailto:M.E.M.Kraakman@lumc.nl),

[C.S.de\\_Brouwer@lumc.nl](mailto:C.S.de_Brouwer@lumc.nl), [I.Sidorov@lumc.nl](mailto:I.Sidorov@lumc.nl), [M.C.W.Feltkamp@lumc.nl](mailto:M.C.W.Feltkamp@lumc.nl), [A.C.M.Kroes@lumc.nl](mailto:A.C.M.Kroes@lumc.nl),

[E.C.J.Claas@lumc.nl](mailto:E.C.J.Claas@lumc.nl), [jjcdevries@lumc.nl](mailto:jjcdevries@lumc.nl)

\*Both authors contributed equally to this work

# Corresponding author

Author contributions: conceptualization: JV, EC, ACMK, methodology: JV, investigation: MK, CB, data analysis: ECC, MK, IS, writing of original draft: ECC, AR, visualization: AR, review and editing: JJCdV, ECJC, ACMK, MCWF

NOTE: This preprint reports new research that has not been certified by peer review and should not be used to guide clinical practice.

## Abstract

### Introduction

Immunocompromised patients are prone to reactivations of multiple latent DNA viruses. Viral load monitoring by single-target quantitative PCRs (qPCR) is the current cornerstone for virus quantification. In this study, a metagenomic next-generation sequencing (mNGS) approach was used for identification and load monitoring of transplantation-related DNA viruses.

### Methods

Longitudinal plasma samples from six patients that were qPCR-positive for cytomegalovirus (CMV), Epstein-Barr virus (EBV), BK polyoma virus (BKV), adenovirus (ADV), parvovirus B19 (B19V), and torque teno-virus (TTV) were sequenced using the quantitative metagenomic Galileo Viral Panel Solution (Arc Bio, LLC) reagents and bioinformatics pipeline combination. Qualitative and quantitative performance was analysed with focus on viral load ranges relevant for clinical decision-making.

### Results

All pathogens identified by qPCR were also identified by mNGS. In addition, BKV, CMV, and HHV6B were detected by mNGS which were not ordered initially but could be confirmed by qPCR. Viral loads determined by mNGS correlated with the qPCR results, with inter-method differences in viral load per virus ranging from 0.19  $\log_{10}$  IU/ml for EBV to 0.90  $\log_{10}$  copies/ml for ADV. TTV, analysed by mNGS in a semi-quantitative way, showed a mean difference of 3.0  $\log_{10}$  copies/ml. Trends over time in viral load determined by mNGS and qPCR were comparable, and clinical thresholds for initiation of treatment were equally indicated by mNGS.

## Conclusion

The Galileo Viral Panel for quantitative mNGS performed comparable to qPCR with regard to detection and viral load determination, within clinically relevant ranges of patient management algorithms.

## Introduction

Opportunistic viral infections frequently occur after solid organ or hematopoietic cell transplantation, with associated morbidity and mortality of up to 40% [1]. Successful prevention and early detection of viral infections including reactivations are the cornerstone of transplant patient management. For effective pre-emptive and therapeutic treatment strategies, accurate viral load quantification is essential. Typically, in immunocompromised hosts, multiple viruses can reactivate simultaneously, which makes comprehensive identification of replicating pathogenic viruses essential. Monitoring of opportunistic viral infections in transplant patients currently most frequently is performed by multiple single-plex quantitative PCRs.

Metagenomic next-generation sequencing (mNGS) is increasingly being applied for the identification of pathogens in undiagnosed cases suspected of an infectious disease [2][3][4]. Quantification of viral loads by means of mNGS remains a challenge [5][6][7][8]. Complicating factors are the varying amount of background sequences from host and bacterial origin, technical bias affecting target sequence depth, unselective attribution of reads, and the amount of calibration curves that are needed simultaneously when using untargeted sequencing for viral load calculations. Reports comparing mNGS with qPCR showed correlation with normalized sequence read counts but never as accurate as qPCR for viral load prediction[5]. Other previous research with regard to quantification of shotgun sequence read counts focused mainly on differential expression of RNA [9][10][11][12]. Recently, the Galileo Viral Panel (Arc Bio, LLC) has been designed as a quantitative mNGS approach for ten transplant-related DNA viruses [13][14]. This all-inclusive approach encompasses the library preparation kit, controls, calibration reagents, and cloud-based user-friendly software for bioinformatic analysis. Previous data on the performance of this mNGS approach showed that the analytical performance was comparable to qPCR results with regard to the limits of detection, limits of quantification, and inter-assay variation [13][14].

In this study, we analysed the performance of the Galileo Viral Panel for longitudinal viral load quantification in transplant patients over time. Subsequent samples from six transplant patients with proven infections or reactivations with transplantation-related DNA viruses (adenovirus, ADV, BK polyomavirus, BKV, cytomegalovirus, CMV, Epstein-Barr virus, EBV, human herpes virus type 6A, HHV-6A, human herpes virus type 6B, herpes simplex type 1, HSV-1, herpes simplex type 2, JC polyomavirus, JC polyomavirus, JCV, varicella zoster virus, VZV, parvovirus B19, B19V, and torque teno virus, TTV) were analysed in comparison with qPCR. Accuracy of viral load quantification by mNGS was studied in relation to thresholds that had been used for the initiation of treatment. Furthermore, we investigated the additional detection of DNA viruses identified by the broad mNGS approach, for which initially no targeted qPCR had been ordered.

## **Methods**

### **Patients and sample selection**

Six immunocompromised patients (one allogeneic stem cell transplant patient, four kidney transplant patients, one haematological patient) were selected based on available follow-up EDTA plasma samples that previously tested positive for one or more transplantation-related DNA viruses. Samples had been previously (July 2008 – December 2019) sent to the Clinical Microbiological Laboratory (CML) of the Leiden University Medical Center (LUMC, The Netherlands) for viral load monitoring. The samples were respectively qPCR positive for ADV, BKV, CMV, EBV, B19V, and TTV, with a wide range of viral loads. Patient plasma samples were stored at -80°C until mNGS analysis.

### **Ethical approval**

Approval was obtained from the ethical committee from the LUMC (P11.165 NL 37682.058.11, and Biobank Infectious Diseases protocol 2020-03 & 2020-04 B20.002).

### **Extraction of nucleic acids, internal controls**

Patient plasma samples were spiked with an internal control (baculovirus, Arc Bio, LLC) prior to extraction. Nucleic acids were extracted from 200 µl plasma using the MagNAPure 96 DNA and Viral NA Small volume extraction kit on the MagNAPure 96 system (Roche Diagnostics, Almere, The Netherlands) with 100 µL output eluate. The eluate was concentrated using vacuum centrifugation by a SpeedVac vacuum concentrator (Thermo Scientific) to a volume of 26 µl.

### **Library preparation and sequencing**

Sequence libraries were prepared using the Galileo Viral Panel sequencing kit (Arc Bio, LLC., Cambridge, MA, USA) according to the manufacturer's instructions. The protocol is based on enzymatic fragmentation at 37°C for 5 minutes, followed by end repair and A-tailing at 65°C for 30

minutes. Subsequently, fragments were ligated using unique dual-index adapters at 20°C for 15 min and purified using magnetic Kapa Pure Beads (Roche). Human DNA was depleted using human depletion reagents at 45°C for 2 hours followed by 45 °C for 15 minutes, after which libraries were amplified using library amplification primers for 45 °C for 30 seconds, by 14 cycles of 98°C for 10 seconds and 65°C for 75 seconds and 65°C for 5 minutes. The final library preparation products were purified using magnetic Kapa Pure Beads (Roche) and quantified using a Qubit fluorometer (Thermo Fisher) followed by equally pooling using the Arc Bio calculation pooling tool. After a final quantity and quality check using a Bioanalyzer (Agilent), samples were sequenced using the NovaSeq6000 sequencing system (Illumina, San Diego, CA, USA) at GenomeScan B.V. (Leiden, the Netherlands) aiming at 10 million reads per library.

### **Calibration samples**

Initial calibration runs were performed testing the multi-analyte mixture (MAM) of whole-virus particles at viral loads of 0, 1,000, 5,000, 10,000, and 100,000 copies/ml or IU/ml plasma, in quintuple (Arc Bio, LLC) for the following 10 viruses: ADV, BKV, CMV, EBV, HHV-6A, HHV6B, HSV-1, HSV-2, JCV, and VZV. For TTV and B19V, no Arc Bio calibrator panels were available, and therefore the Galileo Signal values were plotted against the calibrator plot of other viruses that showed optimal agreement with the viral load (respectively JCV and VZV), representing a semi-quantitative result.

### **Bioinformatic analysis**

After demultiplexing of the sequence reads using bcl2fastq (version), FASTQ files were uploaded to the Galileo Analytics web application [13][15] which automatically processes data for quality assessment and pathogen detection using a custom database of DNA viruses involved in transplant-associated infections: ADV, CMV, EBV, HHV-6A, HHV-6B, HSV-1, HSV-2, JCV, VZV, B19V and TTV. Galileo Analytics web application aligns sequence reads to the genomes of the DNA viruses in their

calibration kit and scores these read alignments based on complexity, uniqueness and alignment scores and reports this in a signal value. The signal value is normalized for read counts across libraries, correcting for differences in genome lengths and technical bias, based on the spiked-in normalization controls. The Signals reported are related to the genomic depth and the observed amount of viral DNA being present in a sample, belonging to non-confounding genomic regions [13]. The sample Signals were visualized in linear calibration curves (**Supplementary Figure 1**).

### **Analysis of performance, and additional findings**

Performance of the metagenomic Galileo Viral Panel assay was assessed in comparison with routine qPCR, analyzing both qualitative and quantitative detection. Additional findings by mNGS were confirmed by additional qPCR analysis. In case no remaining sample was available, the Galileo Analytics software results were compared with results from analysis using alternative bioinformatic tools: metagenomic taxonomic classifier Centrifuge (1.0.4-beta) [16] and *de novo* assembly-based viral metagenomic analysis software Genome Detective [17].



## Results

### Calibration curves

After metagenomic sequencing, the viral loads were calculated for each virus by the Galileo Analytics web application. Signals of both the calibrators and patient plasma samples were plotted in load graphs (**Supplementary Figure 1**) and the corresponding viral load of the patient samples was extrapolated. Since no calibrator panels for B19V and TTV virus were available, these signals were plotted against other calibration curves of viruses that showed the optimal agreement with the known viral load for semi-quantitative detection. All calibration sample signals correlated well with the titer ( $R^2$  range 0.84-0.92).

### Viral load by mNGS versus qPCR

In total six patients were tested by qPCR and mNGS for quantification of different viruses at subsequent time points. Agreement between the methods for qualitative detection was 100% for the viruses targeted by PCR. Quantitative results per patient are shown in **Table 1**, and **Figure 1** depicts viral loads by mNGS versus qPCR per target virus. CMV and EBV viral loads showed highest agreement, with a maximum difference in viral load of 0.70  $\log_{10}$  IU/ml. Mean differences in viral loads were 0.43 for CMV and 0.19  $\log_{10}$  IU/ml for EBV. For ADV, viral loads were higher when quantified with mNGS with a mean difference of 0.90  $\log_{10}$  c/ml. For BKV, viral loads by mNGS were lower in comparison with qPCR, with a mean difference of 1.32  $\log_{10}$  c/ml. When taking into account viral loads measured above the limit of quantification of 2.5  $\log_{10}$  c/ml, as applied in our diagnostic qPCR for BKV, the mean difference is 0.62  $\log_{10}$  c/ml and a trend towards better agreement with higher viral loads could be observed. Semi-quantitative detection of B19V and TTV viruses by mNGS resulted in mean differences of, respectively, 0.39  $\log_{10}$  IU/ml and 3.0  $\log_{10}$  c/ml in comparison with qPCR.

### **Longitudinal patient follow-up and clinical decision-making**

Furthermore, for each patient the viral loads over time were plotted in graphs with clinical information about symptomatology and treatment (**Figure 2**). For CMV, EBV and BKV, in our clinical practice, specific viral load thresholds are used to decide whether immunosuppression should be tapered and/or antiviral therapy should be administered. Viral load quantification around these thresholds showed good agreement in identifying these clinical decision-making breakpoints. In Patient 3, antiviral treatment with foscarnet was started for CMV-reativation when viral load measured by qPCR exceeded  $4.0 \log_{10}$  IU/ml. By mNGS, this critical threshold for treatment initiation was correctly identified with a viral load by mNGS of  $5.44 \log_{10}$  IU/ml. In the same patient, rituximab was administered when the EBV load by qPCR was repeatedly above the threshold of  $4.0 \log_{10}$  IU/ml, consistently quantified thrice above  $4.0 \log_{10}$  IU/ml before administration of rituximab both by qPCR and mNGS.

For B19V, ADV and TTV, no predefined thresholds were used for changing the treatment regimen. For all viruses, the observed trends in load over time in each patient were comparable for qPCR and mNGS, despite the semi-quantitative nature of the B19V mNGS assay. Effect of treatment (anti-viral drugs, immunoglobulins and/or tapering of immunosuppressive drugs) in patients was estimated by follow-up of viral loads by qPCR. For B19V in Patient 5 and 6, the effect of intravenous immunoglobulins (IVIG) could be assessed by the decreasing viral load in the weeks after administration, as observed by mNGS. For ADV, in patient 1, antiviral therapy with cidofovir was started when increasing viral loads were consistently detected, both by qPCR and mNGS.

### **Additional findings**

For some samples additional viral reads were detected in the pathogenic mNGS reports, of viruses that were not initially tested for by qPCR (**Supplementary Table 1**). Most additional findings were supported by a secondary bioinformatic analysis using Centrifuge and Genome Detective: BK (1 patient), CMV (1 patient), HHV-6B (1 patient), and TTV (4 patients). In a few cases, additional

findings were not confirmed by a second analysis leaving some low mNGS signals for CMV, EBV and HSV. JCV was detected by mNGS in a sample with a high concentration of BKV, possibly indicating forced alignment contamination due to high sequence homology between JCV and BKV [13][14].

## Discussion

In this study, the performance of a quantitative mNGS assay for longitudinal follow-up of DNA viral loads was analysed in six immunocompromised patients. Viral loads determined by mNGS were comparable with loads determined by qPCR, and differed less than 1 log<sub>10</sub> for DNA viruses with calibration panels available, in line with previous studies [13][14]. In the current study, the performance of viral loads assessed by mNGS was also evaluated with regard to clinical decision-making. In the management of reactivating viruses in immunocompromised patients, local and international guidelines use viral load breakpoints to decide whether antiviral therapy should be administered or whether immunosuppression should be tapered [18][19][20][21][22]. When local clinical breakpoints were considered for each virus, mNGS performed comparable to qPCR to identify the clinically relevant breakpoints. B19V is not considered to be a reactivating virus, but quantification may be helpful to distinguish clinically relevant replicative infection from merely DNA remnants [23]. In the range of these breakpoints, viral loads were adequately determined by mNGS to guide clinical decision making. Additionally, the longitudinal trend was similar in comparison with qPCR, indicating precision of mNGS for clinical quantification and reliable indication of the trend in viral load. Clinical decision-making is often guided by follow-up of viral load trends, in addition to the cross-sectional viral load measurements for viral infections without available thresholds.

The principle of a quantitative catch-all approach to detect all transplantation-related viruses in a single run is an attractive feature in the clinical follow-up of the immunocompromised host.

Simultaneous reactivation of latent viruses during immunocompromised episodes is common. Co-infection rates of up to 32% have been described using PCR and, importantly, were associated with higher rates of acute rejection or graft dysfunction[24]. Co-infections may be missed when ordering targeted PCRs, while the catch-all approach of mNGS could guarantee that active infections are not overlooked. Indeed, our approach showed a complementary yield of seven reactivating viruses in five patients, which had not been identified earlier by qPCR. Some of these unnoted viruses are not

considered pathogenic, like TTV, which merely reflects the level of functional immunity and could serve as a marker for balancing immunosuppressive treatment [25][26][27]. A significant complementary virus identification yield by mNGS in transplant patients of 31/49 plasma samples was also reported by Sam et al [14], with the majority being viruses considered pathogenic. These findings show that mNGS could improve pathogen detection in clinical practice.

Another advantage of mNGS would be its capacity to genotype viruses and detect mutations associated with antiviral resistance, without the need for additional, time consuming, target-specific ‘wet’ lab procedures that could delay diagnosis and treatment. As an example, Patient 3 in our study was treated with foscarnet for persistent CMV reactivation pending the results of mutational analysis after clinical failure of valganciclovir treatment. If the results of mutational analysis had been immediately available, resorting to second-line treatment may have been avoided.

Widespread implementation of mNGS approaches in clinical diagnostic settings has been limited by several factors. The ‘wet’ lab protocols can be time-consuming, costly, and have a relatively long turnaround time mainly due to the time required for sequencing. With various sequencing techniques still rapidly evolving, the costs and sequencing turnaround time of such protocols is expected to improve considerable in the future [28]. Furthermore, bioinformatic skills are generally needed for validation and implementation as a diagnostic assay. User-friendly, all-in one mNGS data-analysis software packages for cloud-based, automated analysis, enables use in laboratories with minimal bioinformatic knowledge and high-performance computing capacity.

Limitations in this current study are the relatively low number of samples and viruses when considering a metagenomic approach, including two viruses without calibration panels available. This small-scale study provides a proof-of-principle demonstration in a retrospective design that the current version of the Research Use Only Galileo Viral Panel enables longitudinal viral load monitoring by mNGS. It is expected that after these initial studies indicating high performance in terms of limit of detection and quantification, inter-run precision and prospective viral load monitoring, the kit and software will be expanded to include more viruses, calibration samples and

potentially fit for different sample types. Furthermore, technical and bioinformatic features might be evolved in future versions of the assay.

Overall, viral metagenomic sequencing is a promising approach not only DNA virus detection and identification, but also for reliable estimation of the viral load in a clinical setting, and potentially mutational typing for drug sensitivity analysis. Several milestones essential for implementation in diagnostics settings have been met by the specific assay used in this study: the limits of detection, the limits of quantification, precision and overall technical performance, which were comparable with qPCR assays. Precise quantification was accomplished by read normalization based on a designed control. These accomplishments pave the way for further developments and optimization of quantitative metagenomic sequencing for longitudinal viral load monitoring and beyond.

### **Acknowledgements**

We thank Gavin Wall, Naissan Hussainzada, and Meredith Carpenter (Arc Bio) for their technical and logistic support.

### **Conflict of interest**

None

## References

- [1] I. G. Sia and R. Patel, 'New Strategies for Prevention and Therapy of Cytomegalovirus Infection and Disease in Solid-Organ Transplant Recipients', *Clin. Microbiol. Rev.*, vol. 13, no. 1, pp. 83–121, Jan. 2000, doi: 10.1128/CMR.13.1.83.
- [2] E. C. Carbo *et al.*, 'Improved diagnosis of viral encephalitis in adult and pediatric hematological patients using viral metagenomics', *J. Clin. Virol.*, p. 104566, Jul. 2020, doi: 10.1016/j.jcv.2020.104566.
- [3] A. Reyes *et al.*, 'Viral metagenomic sequencing in a cohort of international travellers returning with febrile illness', *Infectious Diseases (except HIV/AIDS)*, preprint, May 2021. doi: 10.1101/2021.05.13.21257019.
- [4] A. L. van Rijn *et al.*, 'The respiratory virome and exacerbations in patients with chronic obstructive pulmonary disease', *PLOS ONE*, vol. 14, no. 10, p. e0223952, Oct. 2019, doi: 10.1371/journal.pone.0223952.
- [5] S. van Boheemen *et al.*, 'Retrospective Validation of a Metagenomic Sequencing Protocol for Combined Detection of RNA and DNA Viruses Using Respiratory Samples from Pediatric Patients', *J. Mol. Diagn.*, vol. 22, no. 2, pp. 196–207, Feb. 2020, doi: 10.1016/j.jmoldx.2019.10.007.
- [6] J. J. C. de Vries *et al.*, 'Benchmark of thirteen bioinformatic pipelines for metagenomic virus diagnostics using datasets from clinical samples', *J. Clin. Virol.*, p. 104908, Jul. 2021, doi: 10.1016/j.jcv.2021.104908.
- [7] F. X. López-Labrador *et al.*, 'Recommendations for the introduction of metagenomic high-throughput sequencing in clinical virology, part I: Wet lab procedure', *J. Clin. Virol.*, vol. 134, p. 104691, Jan. 2021, doi: 10.1016/j.jcv.2020.104691.
- [8] J. J. C. de Vries *et al.*, 'Recommendations for the introduction of metagenomic next-generation sequencing in clinical virology, part II: bioinformatic analysis and reporting', *J. Clin. Virol.*, vol. 138, p. 104812, May 2021, doi: 10.1016/j.jcv.2021.104812.
- [9] G. Cai *et al.*, 'Accuracy of RNA-Seq and its dependence on sequencing depth', *BMC Bioinformatics*, vol. 13, no. Suppl 13, p. S5, 2012, doi: 10.1186/1471-2105-13-S13-S5.
- [10] C. Trapnell, D. G. Hendrickson, M. Sauvageau, L. Goff, J. L. Rinn, and L. Pachter, 'Differential analysis of gene regulation at transcript resolution with RNA-seq', *Nat. Biotechnol.*, vol. 31, no. 1, pp. 46–53, Jan. 2013, doi: 10.1038/nbt.2450.
- [11] K. R. Kukurba and S. B. Montgomery, 'RNA Sequencing and Analysis', *Cold Spring Harb. Protoc.*, vol. 2015, no. 11, p. pdb.top084970, Nov. 2015, doi: 10.1101/pdb.top084970.
- [12] C. Y. Chiu *et al.*, 'Diagnosis of Fatal Human Case of St. Louis Encephalitis Virus Infection by Metagenomic Sequencing, California, 2016', *Emerg. Infect. Dis.*, vol. 23, no. 10, pp. 1964–1968, Oct. 2017, doi: 10.3201/eid2310.161986.
- [13] M. L. Carpenter *et al.*, 'Metagenomic Next-Generation Sequencing for Identification and Quantitation of Transplant-Related DNA Viruses', *J. Clin. Microbiol.*, vol. 57, no. 12, pp. e01113-19, /jcm/57/12/JCM.01113-19.atom, Sep. 2019, doi: 10.1128/JCM.01113-19.
- [14] S. S. Sam, R. Rogers, F. S. Gillani, G. J. Tsongalis, C. S. Kraft, and A. M. Caliendo, 'Evaluation of a Next-Generation Sequencing Metagenomics Assay to Detect and Quantify DNA Viruses in Plasma from Transplant Recipients', *J. Mol. Diagn.*, vol. 23, no. 6, pp. 719–731, Jun. 2021, doi: 10.1016/j.jmoldx.2021.02.008.
- [15] 'ArcBio Galileo Transplant WebApp'. [Online]. Available: [galileo.arcbio.com](http://galileo.arcbio.com)
- [16] D. Kim, L. Song, F. P. Breitwieser, and S. L. Salzberg, 'Centrifuge: rapid and sensitive classification of metagenomic sequences', *Genome Res.*, vol. 26, no. 12, pp. 1721–1729, Dec. 2016, doi: 10.1101/gr.210641.116.
- [17] M. Vilsker *et al.*, 'Genome Detective: an automated system for virus identification from high-throughput sequencing data', *Bioinformatics*, vol. 35, no. 5, pp. 871–873, Mar. 2019, doi: 10.1093/bioinformatics/bty695.

- [18] R. R. Razonable and A. Humar, 'Cytomegalovirus in solid organ transplant recipients—Guidelines of the American Society of Transplantation Infectious Diseases Community of Practice', *Clin. Transplant.*, vol. 33, no. 9, Sep. 2019, doi: 10.1111/ctr.13512.
- [19] H. H. Hirsch, P. S. Randhawa, and AST Infectious Diseases Community of Practice, 'BK polyomavirus in solid organ transplantation—Guidelines from the American Society of Transplantation Infectious Diseases Community of Practice', *Clin. Transplant.*, vol. 33, no. 9, Sep. 2019, doi: 10.1111/ctr.13528.
- [20] T. Lion, 'Adenovirus persistence, reactivation, and clinical management', *FEBS Lett.*, vol. 593, no. 24, pp. 3571–3582, Dec. 2019, doi: 10.1002/1873-3468.13576.
- [21] Manaresi and Gallinella, 'Advances in the Development of Antiviral Strategies against Parvovirus B19', *Viruses*, vol. 11, no. 7, p. 659, Jul. 2019, doi: 10.3390/v11070659.
- [22] U. D. Allen, J. K. Preiksaitis, and the AST Infectious Diseases Community of Practice, 'Post-transplant lymphoproliferative disorders, Epstein-Barr virus infection, and disease in solid organ transplantation: Guidelines from the American Society of Transplantation Infectious Diseases Community of Practice', *Clin. Transplant.*, vol. 33, no. 9, Sep. 2019, doi: 10.1111/ctr.13652.
- [23] M. W. A. Molenaar-de Backer, A. Russcher, A. C. M. Kroes, M. H. G. M. Koppelman, M. Lanfermeijer, and H. L. Zaaijer, 'Detection of parvovirus B19 DNA in blood: Viruses or DNA remnants?', *J. Clin. Virol.*, vol. 84, pp. 19–23, Nov. 2016, doi: 10.1016/j.jcv.2016.09.004.
- [24] C. Anderson-Smits, E. R. Baker, and I. Hirji, 'Coinfection rates and clinical outcome data for cytomegalovirus and Epstein-Barr virus in post-transplant patients: A systematic review of the literature', *Transpl. Infect. Dis.*, vol. 22, no. 6, Dec. 2020, doi: 10.1111/tid.13396.
- [25] S. Spandole, D. Cimponeriu, L. M. Berca, and G. Mihăescu, 'Human anelloviruses: an update of molecular, epidemiological and clinical aspects', *Arch. Virol.*, vol. 160, no. 4, pp. 893–908, Apr. 2015, doi: 10.1007/s00705-015-2363-9.
- [26] A. Moustafa *et al.*, 'The blood DNA virome in 8,000 humans', *PLOS Pathog.*, vol. 13, no. 3, p. e1006292, Mar. 2017, doi: 10.1371/journal.ppat.1006292.
- [27] A. L. van Rijn *et al.*, 'Torque teno virus loads after kidney transplantation predict allograft rejection but not viral infection', *J. Clin. Virol.*, vol. 140, p. 104871, Jul. 2021, doi: 10.1016/j.jcv.2021.104871.
- [28] A. von Bubnoff, 'Next-Generation Sequencing: The Race Is On', *Cell*, vol. 132, no. 5, pp. 721–723, Mar. 2008, doi: 10.1016/j.cell.2008.02.028.



**Table 1.** Viral load quantification by qPCR and mNGS per patient sample.

Patient-sample	Virus	Viral load qPCR	Viral load qPCR (log <sub>10</sub> )	Viral load mNGS	Viral load mNGS (log <sub>10</sub> )	ΔqPCR-mNGS (log <sub>10</sub> )
P1-S1	ADV	675 c/mL	2,83 c/mL	1277 c/mL	3,11 c/mL	0,28 c/mL
P1-S2		4517	3,65	66273	4,82	1,17
P1-S3		34740	4,54	287844	5,46	0,92
P1-S4		136900	5,14	1435130	6,16	1,02
P1-S5		60540	4,78	777172	5,89	1,11
P2-S1	BKV	796 c/mL	2,90 c/mL	3 c/mL	0,48 c/mL	-2,42 c/mL
P2-S2		614	2,79	3	0,48	-2,31
P3-S3		233700	5,37	9011	3,95	-1,41
P4-S4		2401000	6,38	1857785	6,27	-0,11
P5-S5		71480	4,85	32321	4,51	-0,34
P3-S1	CMV	2370 IU/mL	3,37 IU/mL	6246 IU/mL	3,80 IU/mL	0,42 IU/mL
P3-S2		122800	5,09	275657	5,44	0,35
P3-S3		10680	4,03	22242	4,35	0,32
P3-S4		4915	3,69	11366	4,06	0,36
P3-S5		9156	3,96	46231	4,66	0,70
P3-S1	EBV	2083 IU/mL	3,32 IU/mL	4581 IU/mL	3,66 IU/mL	0,34 IU/mL
P3-S2		12970	4,11	1573	4,20	0,09
P3-S3		17710	4,25	14549	4,16	-0,09
P3-S4		10500	4,02	15077	4,18	0,16
P3-S5		7723	3,89	14844	4,17	0,28
P4-S1	TTV*	140 c/mL	2,15 c/mL	4 c/mL	0,60 c/mL	-1,54 c/mL
P4-S2		2400000	6,38	5142	3,71	-2,67
P4-S3		5,7E+09	9,76	319074	5,50	-4,25
P4-S4		2,4E+08	8,38	46261	4,67	-3,71
P5-S1	B19V*	1,34E+11 IU/mL	11,13 IU/mL	2,07E+11 IU/mL	11,32 IU/mL	0,19 IU/mL
P5-S2		1407365	6,15	1235416	6,09	-0,06
P5-S3		45846	4,66	41787	4,62	-0,04
P6-S1	B19V*	4,07E+10 IU/mL	10,61 IU/mL	4,37E+11 IU/mL	11,64 IU/mL	1,03 IU/mL
P6-S2		5309308	6,73	9376953	6,97	0,25
P6-S3		8569	3,93	49601	4,70	0,76

\*B19V and TTV results were considered semi-quantitative since no Arc Bio calibration samples were available for these targets.

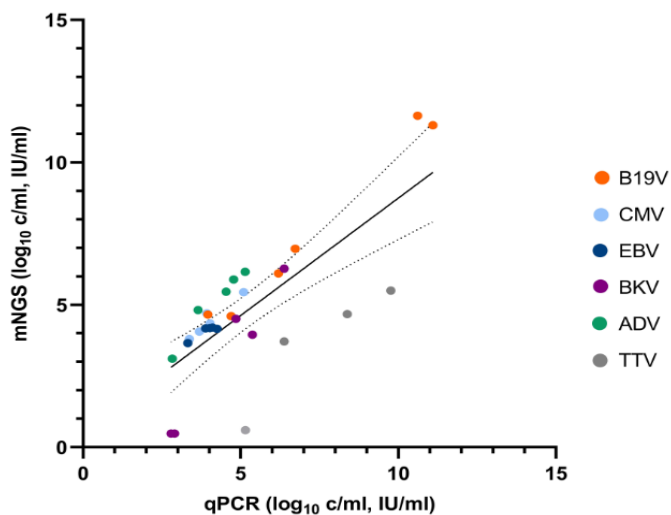


**Figure 1.** Viral loads as predicted by Galileo Viral Panel mNGS versus qPCR (copies/ml for ADV, BK, and TTV, and IU/ml for CMV, EBV and B19V). B19V and TTV results were considered semi-quantitative since no Galileo calibration panels were available for these targets.

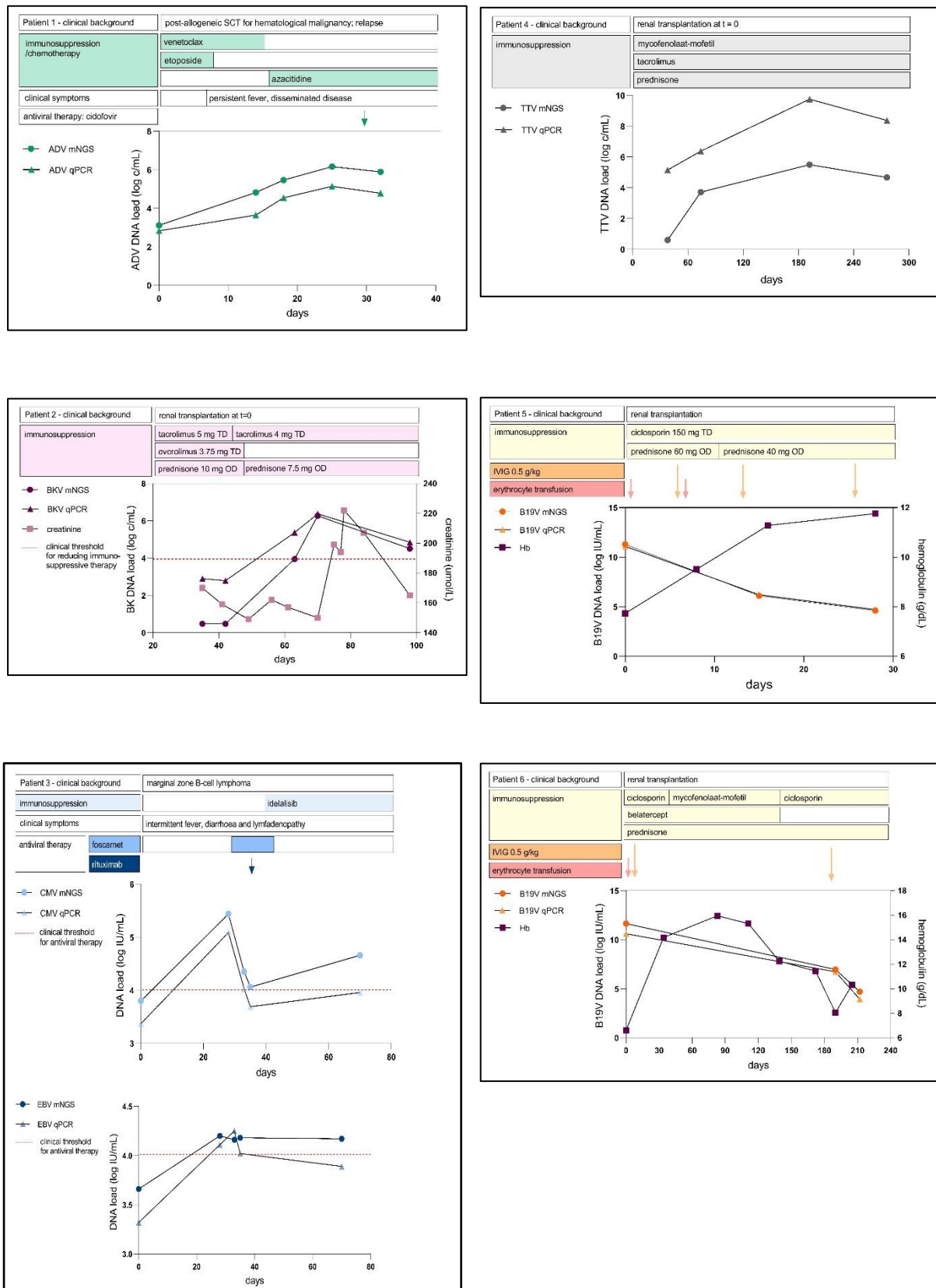
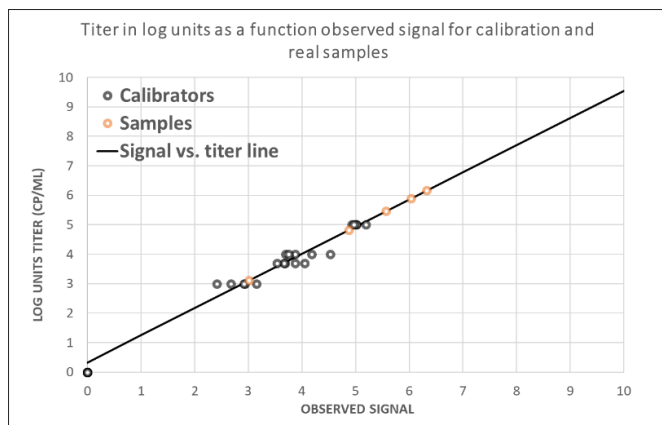
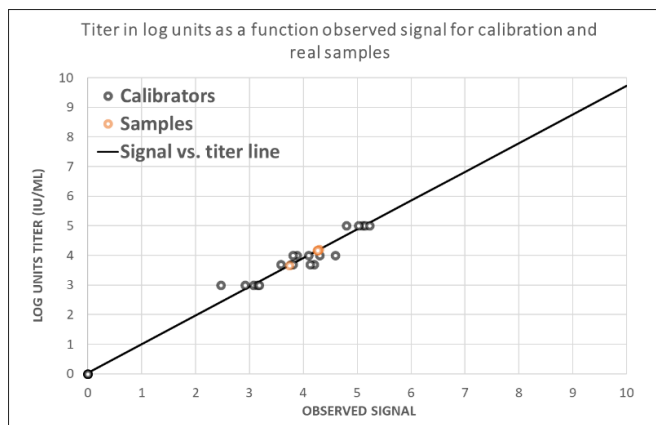


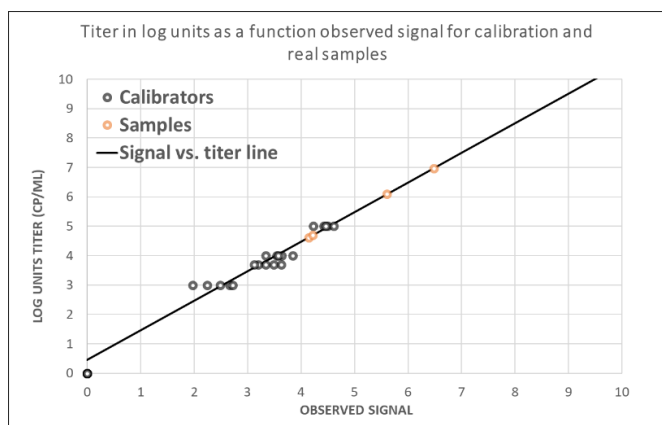
**Figure 2.** Longitudinal follow-up of DNA viral loads in immunosuppressed patients over time, as predicted by mNGS (Galileo Viral Panel, Arc Bio) versus qPCR. Clinical information and therapeutic agents are included.



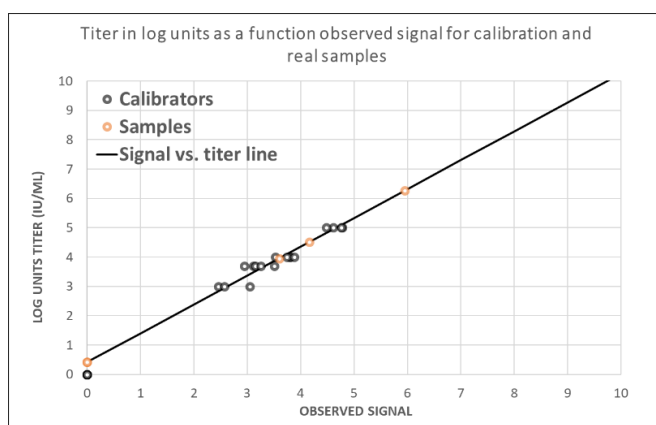
ADV; slope=0.92, intercept=0.33,  $R^2=0.92$



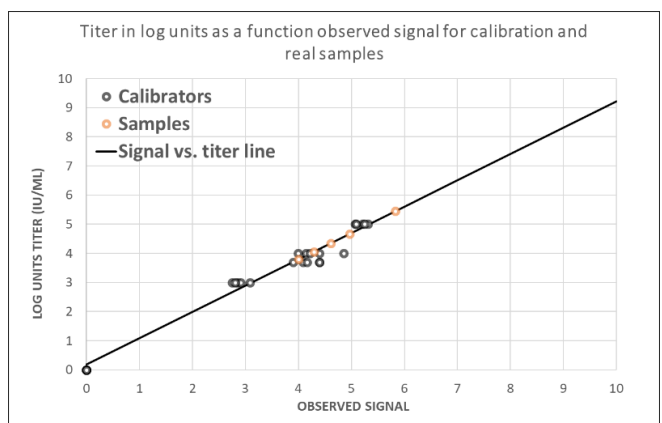
EBV; slope=0.97, intercept=0.04,  $R^2=0.9$



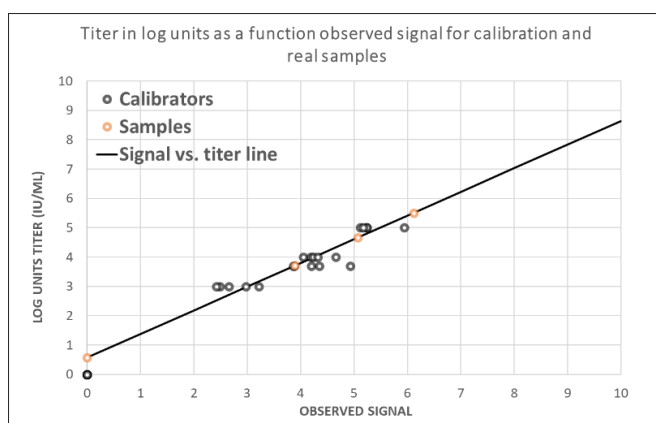
B19V; slope=1.01, intercept=0.45,  $R^2=0.91$



BKV; slope=0.98, intercept=0.42,  $R^2=0.92$



CMV; slope=0.9, intercept=0.18,  $R^2=0.89$



TTV; slope=0.81, intercept=0.57,  $R^2=0.84$

**Supplementary Figure 1.** Calibration graphs of the six viruses in six patients in this study with associated slope, intercepts and  $R^2$  values. Concentrations are expressed in  $\log_{10}$  copies or IU/ml. Calibrator samples are shown in black dots, clinical samples in orange.

**Supplementary Table 1.** Additional findings of the metagenomic Galileo Viral Panel compared to Centrifuge and Genome Detective software. For Galileo Analytics, results are presented as viral load in log<sub>10</sub> c/mL or IU/ml. For Centrifuge and Genome Detective, results are presented as absolute amount of reads classified per species or genus. For TTV reads during centrifuge analysis, Anelloviridae reads are shown.

P1 ADV		S1	S2	S3	S4	S5
BKV	Galileo Analytics		3.67	4.03	3.78	
	Centrifuge		47	74	67	
	Genome Detective		84	113	35	
CMV	Galileo Analytics	2.45	3.69	3.84	3.84	3.16
	Centrifuge	18	123	83	53	1
	Genome Detective	0	12	156	2	0
EBV	Galileo Analytics		1.22			
	Centrifuge		0			
	Genome Detective		0			
B19V	Galileo Analytics	3.85	3.65		3.55	
	Centrifuge	0 (1 AADPA <sup>†</sup> )	2 (147 AADPA)		0 (1 AADPA)	
	Genome Detective	0	(140 AAV2 <sup>‡</sup> )		(124 AAV2)	
TTV	Galileo Analytics	5.54	6.18	4.98	4.61	4.39
	Centrifuge	2382	3525	489	137	2
	Genome Detective	11426	22595	2719	823	2

<sup>†</sup> AADPA = Adeno-associated dependoparvovirus A; <sup>‡</sup>AAV2 = adeno-associated virus 2

P2 BKV		S1	S2	S3	S4	S5
ADV	Galileo Analytics	2.94		2.94		2.44
	Centrifuge	3		0		1
	Genome Detective	0		0		0
CMV	Galileo Analytics		2.6	4.46	5.07	
	Centrifuge		13	279	1056	
	Genome Detective			110	975	
TTV	Galileo Analytics	3.87	4.84	5.54	4.71	4.99
	Centrifuge	96	1196	953	56	1511
	Genome Detective	406	7037	5900	241	11141
VZV	Galileo Analytics			2.3		
	Centrifuge			1		
	Genome Detective			0		
JCV	Galileo Analytics				4.06	
	Centrifuge				0	
	Genome Detective				0	
HSV	Galileo Analytics		0.87			
	Centrifuge		1			
	Genome Detective					

P3 CMV/EBV		S1	S2	S3	S4	S5
BKV	Galileo Analytics		4.99	4.98	4.89	5.12
	Centrifuge		22	60	33	21
	Genome Detective		0	38	4	0
B19V	Galileo Analytics	4.69	4.93	5.52	5.16	5.17
	Centrifuge	0	1	0	1	2
	Genome Detective	0	0	0	0	0
TTV	Galileo Analytics	5.21		5.19	5.25	5.66
	Centrifuge	22		45	35	131
	Genome Detective	37		168	97	547
HHV6A	Galileo Analytics		3.48			
	Centrifuge		1			
	Genome Detective		0			
HHV6B	Galileo Analytics		4.11			
	Centrifuge		14			
	Genome Detective		14			

P4 TTV		S1	S2	S3	S4
CMV	Galileo Analytics	2.95	3.46		
	Centrifuge	26	38		
	Genome Detective	28	53		
B19V	Galileo Analytics	3.98	4.16	4.07	4.27
	Centrifuge	2	1	1	3
	Genome Detective	0	0	0	0

P5 B19V		S1	S2	S3
CMV	Galileo Analytics	2.71		3.46
	Centrifuge	2		27
	Genome Detective	4		52
EBV	Galileo Analytics		2.08	
	Centrifuge		0	
	Genome Detective		0	
BKV	Galileo Analytics			3.81
	Centrifuge			12
	Genome Detective			20
HSV1	Galileo Analytics			3.25
	Centrifuge			12
	Genome Detective			0
HSV2	Galileo Analytics			2.76
	Centrifuge			0
	Genome Detective			0

P6 B19V		S1	S2	S3
ADV	Galileo Analytics			2.72
	Centrifuge			1
	Genome Detective			0
EBV	Galileo Analytics		1.19	
	Centrifuge		0	
	Genome Detective		0	
TTV	Galileo Analytics	6.58	2.83	2.70
	Centrifuge	1681	10094	3
	Genome Detective	10100	17873	0